UNIVERSITY OF CALIFORNIA, SAN DIEGO

Detecting Abl Tyrosine Kinase in Mouse Tissues

A thesis submitted in partial satisfaction of the
requirements for the degree Master of Science

in

Biology

by

Amini Hwang

Committee in charge:

Professor Jean Y.J. Wang, Chair
Professor Jens Lykke-Andersen, Co-Chair
Professor Michael David

2015

The thesis of Amini Hwang is approved, and it is acceptable in quality and form for publication on microfilm and electronically:

Co-Chair

Chair

University of California, San Diego

2015

DEDICATION

I would like to dedicate this to everyone who has helped me come this far.

TABLE OF CONTENTS

LIST OF FIGURES

ACKNOWLEDGEMENTS

I would like to thank Dr. Wang for allowing me to work in her lab, and not giving up on this mess of a student. It was through her counseling and teaching that I was able to come this far.

I would like to thank Dr. Shuhbra Rastogi for helping me the last few months with many experiments, writing, and showing me angelic patience.

I would like to thank Dr. Eric Tu for all the training, math, clean lab habits, and for teaching me immunofluorescence.

I would like to thank Dr. Priya Sridevi for helping me understand concepts and calculations, and for making lab conversations very interesting.

I would like to thank Chet, Daniel, Edison, Ritesh, and Elaine for all the good conversations that have kept me awake, the homemade food or coffee runs, dilution calculations, and for being so encouraging.

I would finally like to thank Dr. Jens Lykke-Andersen and Dr. Michael David for serving on my committee.

Thank you so much.

ABSTRACT OF THE THESIS

Detecting Abl Tyrosine Kinase in Mouse Tissues

by

Amini Hwang

Master of Science in Biology

University of California, San Diego, 2015

Professor Jean Y.J. Wang, Chair

Professor Jens Lykke-Andersen, Co-Chair

Abl tyrosine kinase is a ubiquitously expressed non-receptor tyrosine kinase that undergoes constant nucleocytoplasmic shuttling. In response to DNA damage, Abl localizes and is activated in the nucleus to stimulate intrinsic apoptosis. Whereas in response to growth factors, Abl localizes and is activated in the cytoplasm to regulate actin dynamics. Depending on the subcellular localization of where Abl is activated, Abl decides the fate of the cell, making its visualization both useful and vital. Here we show the optimal immunofluorescence method to detect Abl in mouse tissues. Using this method, we have observed that WT mouse testis tissues express nuclear Abl in spermatid heads without DNA-damaging agents. We have also found that cisplatin treatments induce nuclear localization of Abl in Abl-WT mouse spleen and testis tissues, but not in Abl- μNLS mouse spleen and testis tissues. Due to the heterogeneity of cells expressing nuclear Abl in response to DNA damage, we

hypothesized that Abl accumulates in the nucleus only in proliferating cells in response to DNA damage. So far, we have found that in response to DNA damage, Abl accumulates in the nucleus only in proliferating 3T3 WT cells.

I.

Introduction

Abl Tyrosine Kinase

Abl tyrosine kinase is a ubiquitously expressed non-receptor tyrosine kinase that is 123-kDa. Similar to other nonreceptor tyrosine kinases, it has the characteristic kinase domain and Src homology domains, SH3 and SH3 (Wang, 2000). Unlike other nonreceptor tyrosine kinases, however, Abl tyrosine kinase is found both in the cytoplasm and nucleus. It has sequences in its C terminal region that contain three nuclear localization signals (NLS), a nuclear export signal (NES), a DNA-binding domain (DBD), and an F-actin binding domain (14).

Upon exposure to DNA-damaging agents such as cisplatin, doxorubicin, and ionizing radiation (IR), there is an accumulation and activation of nuclear Abl through ATM and DNA-PK dependent mechanisms (1, 7, 3). The activated nuclear Abl will then stimulate intrinsic apoptosis by triggering the p53 and p73 family of transcription factors (8, 1).

NLS and NES

The NLS and NES sequences allow Abl to shuttle between the nucleus and cytoplasm; the three NLS import Abl into the nucleus whereas the NES actively exports Abl into the cytoplasm (14). In response to growth factors, cytokines (i.e. TNFα), extracellular matrix proteins, and microbial infections, Abl localizes and is activated in the cytoplasm where it regulates actin dynamics (12). In response to DNA damage, Abl localizes and is activated in the nucleus where it then regulates gene expression and DNA repair (5).

Leptomycin B

Leptomycin B (LMB) inactivates the NES-receptor, CRM1/exportin1 (9). Inactivating the NES-receptor, exportin1, results in nuclear accumulation of Abl. It has been established that 3T3 Abl-WT cells express an even distribution of Abl throughout the cytoplasm and nucleus, but with LMB treatment the 3T3 Abl-WT cells express higher expression of nuclear Abl (9). Previous studies have shown that active oncogenic BCR-Abl is exclusively cytoplasmic (14). Furthermore, it has been established that nuclear entrapment of the oncogenic BCR-Abl through application of imatinib (a kinase inhibitor that induces entry of nuclear BCR-Abl) and LMB will convert the oncogene, so as to induce apoptosis (13).

Abl- μNLS mice and Abl null mice

It is difficult to study Abl's apoptotic function *in vivo* due to Abl null mice resulting in embryonic or neonatal lethality (10). To study Abl's apoptotic function, our lab has generated healthy and fertile Abl- μNLS mice, where all three nuclear localization signals have been rendered inactive by replacing the sequences with mutated cDNA (5, 8).

Immunofluorescence

Immunofluorescence is a widely used, microscope-based technique that uses fluorescent-labeled antibodies to detect specific proteins of interest (4). This technique is comprised of the basic template: fixation, permeabilization, blocking, and the application of primary and secondary antibodies. Fluorescence quality is

crucial for an accurate expression of protein of interest. Several factors may influence fluorescence quality: proper specimen care, modification of each immunofluorescence-template component so that it may be appropriate in concentration, strength (type of reagent), and speed (time and temperature), etc. For example, fixation with glutaraldehyde provides the best preservation of fine cellular structures but is infamous for its autofluorescence, leading to poor image quality. The popular tissue fixation with methanol gives high image clarity because it does not utilize chemical cross linking, but results in flattening and poor preservation of the tissue structure due to protein and carbohydrate precipitation. Ultimately, this powerful visualization technique has limitations, and a more tailored approach must be made for each use-case (specific to what must be optimized) with these goals in mind: preservation of cellular structure, antigen accessibility, and an accurate expression and distribution of the chosen antigen as close as possible to its *in vivo* state.

II.

Results

Cell Pellet Sections

Having no Abl - / - mice tissue, cell pellet sections were made to mimic tissue. Cell pellets are thicker in sample size and can be used as controls to test different antibody dilutions and antigen retrieval methods (2). Cell pellets were made for 3T3 Abl +/+, 3T3 Abl -/-, 3T3 Abl +/+ treated with LMB, and 3T3 Abl -/- treated with LMB by growing 100 million cells of each phenotype and treating them with either vehicle or LMB. Cells were spun into pellets, embedded in optimal cutting temperature compound (OCT), snap frozen, and then sectioned (5 μm thick) onto microscope slides. The same lab protocol used to detect Abl in 3T3 Abl-WT and 3T3 Abl-KO monolayer cells was applied on cell pellet sections and resulted in low fluorescence quality. For 3T3 Abl-WT and 3T3 Abl-KO cell pellet sections, the following protocol detected Abl: 2% PFA fixation for 10 minutes at room temperature, 70% ethanol post fixation for 10 minutes at room temperature, followed by 0.5% Triton X-100 permeabilization for 10 minutes at room temperature (Figure 1). Corresponding to previous published data (9), 3T3 Abl-WT cells expressed both nuclear and cytoplasmic Abl (Figure 1 Panel B,C). With LMB treatment, which inactivates the NES-receptor CRM1/export1, there was accumulation of nuclear Abl (Figure 1 Panel H, I).

Tissue

The previous lab protocol used the following method to preserve tissue after harvest: embedding the organs in 100% OCT, then snap freezing the OCT molds in isopentane over dry ice, followed by cutting the molds into 5- μm sections onto microscope slides for immunofluorescence. Using the fixation and

permeabilization method appropriate for cell pellet sections resulted in poor tissue structure preservation (Figure 2A). Having assumed that it was due to poor fixation and permeabilization method, several other methods were executed and came to similar results: poor tissue structure preservation, large spaces and holes throughout the tissue, and high background fluorescence (Figure 2B).

A different protocol was made to prevent both poor tissue structure preservation and the large spaces and holes within the tissues. After mice were treated with cisplatin for 2 hours, the organs were harvested and immediately placed into cold PBS. Kidneys were cut in halves and all other organs were cut into approximately the same size as halves of kidneys. Knowing that 4% PFA penetrates ~2 mm/ 1 hour in RT and the volume of each cut organ, each organ was placed in 500 µL of freshly prepared 4% PFA for 16 hours RT. Following fixation, the organs were placed in 15% sucrose in PBS solution for 24 hours at 4° C. They were then transferred into 30% sucrose in PBS solution for 24 hours at 4° C. Sucrose prevents the formation of ice crystals within frozen tissue sections, freezes approximately at the same speed and hardness as paraformaldehyde fixed tissue providing optimal cryoprotection. The succession of increasing sucrose concentrations counteracts not only osmotic shock but also delivers thorough diffusion. After the 24 hours, half of the 30% sucrose solution was replaced with 30% OCT in PBS for 2 hours at 4° C, this solution facilitates OCT penetration. Finally, the organs were embedded in 100% OCT for 1 hour at 4° C (cutting the OCT bottle wider at the opening and placing the OCT in all vinyl molds at once prevents the formation of bubbles). The OCT embedded organs

were then placed slowly into a bath with crushed dry ice and isopentane. Holding the molds with forceps, they were frozen from bottom to top.

To ensure that signal was not autofluorescence, the following controls were endeavored: primary antibody only (monoclonal 8E9 anti-mouse), secondary antibody only (Alexa Fluor 488 chicken anti-mouse), and 5% BSA only. All controls expressed minimum to no fluorescence.

Another source of autofluorescence is natural fluorescence. Natural fluorescence arises from several components of tissues: flavins and porphyrins, elastin, collagen, laminin, and lipofuscin (6). Sudan Black B, a lysochrome or fat soluble dye, is used to diminish natural fluorescence. Lipofuscin, for example, is an accumulation of lysosomes and the pigment from old blood cells gives rise to natural fluorescence. Sudan Black B will stain lipofuscin blue black, thus decreasing the natural fluorescence. Tissue sections stained with 0.1% Sudan Black B exhibited decreased fluorescence overall (Figure 3).

Abl Expression in Mouse Testis Tissue

With the previously stated controls satisfied, mouse testis tissues were stained for Abl, DNA, and F-actin. Tissue sections were placed into room temperature PBS for 15 minutes, then permeabilized with 0.5% Triton X-100 for 15 minutes. Tissue sections were then blocked with 5% BSA. Abl was stained with anti-Abl 8E9 antibody, DNA was stained with Hoechst DNA dye, and F-actin was stained with Phalloidin Alexa Fluor 594. Tissue sections exhibited no holes and structural components such as individual seminiferous tubules could be identified (Figure 4A, 4B).

Abl μNLS mice testis tissue exhibited cytoplasmic Abl in all stages of spermatogenesis (Figure 5 Panel B). Spermatid tails had Abl expression, which co-localized with F-actin (Figure 7). There was also high expression of Abl in the basement membrane of all seminiferous tubules. Cisplatin treated Abl μNLS mice testis tissue exhibited similar Abl expression distribution as untreated Abl μNLS mice testis tissue (Figure 5 Panel B and F).

Abl-WT mouse testis tissue, untreated, expressed mostly cytoplasmic Abl in all cells, but spermatid heads expressed nuclear Abl (Figure 6 Panel B, Figure 7). Cisplatin treated Abl-WT mouse testis tissue expressed higher nuclear Abl fluorescence in spermatid heads, and also expressed nuclear Abl in spermatogonia and spermatocytes.

Abl Expression in Mouse Spleen Tissue

Abl-WT and Abl- μNLS mouse spleen tissues were stained for Abl and DNA. Abl-WT, Abl- μNLS, and cisplatin treated Abl- μNLS mouse spleen tissue cells expressed only cytoplasmic Abl (Figure 8). Cisplatin treated Abl-WT spleen tissue, however, comprised cells that express nuclear Abl (Figure 8). To confirm that the nuclear Abl expression is within the nucleus and is not background fluorescence (Abl expression from cells below or behind cell of interest), z-stack images were taken of both Abl- μNLS spleen tissue and Abl-WT spleen tissue. The z-stack images encompass of 41-45 slices, each slice 0.30 μm deep. The compilation displays the spleen cells from the sides (yz and xz axis). Both the yz and xz axis views show that Abl- μNLS spleen cells have no nuclear Abl (Figure

9A). In Abl-WT spleen cells, there is nuclear Abl in 2/3 cells in the yz panel and 1/3 cells in the xz panel (Figure 9B).

Based on the heterogeneity of cells that express nuclear Abl in both cisplatin treated Abl-WT spleen tissue and cisplatin treated Abl-WT testis tissue, we hypothesized that in response to DNA damage, Abl accumulates in the nucleus only in proliferating cells. To investigate, 3T3 monolayer cells were chosen as the experimental system.

Effect of Radiation on Ki67 Expression in Abl-WT 3T3 Fibroblasts

In steady state Abl-WT 3T3 fibroblasts, Abl is expressed in both cytoplasm and nucleus. In steady state Abl- μNLS 3T3 fibroblasts, there is expression of only cytoplasmic Abl (Figure 10). Before continuing onto our experimental strategy, we first observed the effects of radiation on Abl localization in Abl-WT and Abl-μNLS 3T3 cells. In Abl- μNLS cells, there is exclusive cytoplasmic Abl localization upon irradiation. Most Abl- WT cells without ionizing radiation show both cytoplasmic and nuclear localization of Abl. With radiation 2.5 Gy, there is a 25% increase in the number of cells showing C=N expression of Abl. With radiation of 10 Gy, there is an increase in the number of cells with C=N Abl expression by 30%. With increasing doses of ionizing radiation, we have an increase in the number of cells that express nuclear Abl (Figure 11B).

Our experimental strategy was to have one group of 3T3 Abl- WT cells receive an initial ionizing radiation dosage of 10 Gy and after five days of culture, they would receive a final dosage of another 10 Gy (to induce DNA damage and thus accumulation of nuclear Abl). We had another group of 3T3 Abl- WT cells

that received a dosage of 2.5 Gy then after 5 days of culture they received a 10 Gy dosage. All cells were stained for Ki67, a marker for proliferating cells, which is present during all active phases of cell cycle but is absent in resting cells. Cells were also stained for Abl and counterstained with Hoechst DNA dye. The control group of 3T3 Abl-WT cells that were not irradiated expressed 82% of Ki67+ cells, whereas the group that underwent 2.5 Gy then a final dosage of 10 Gy five days later expressed 46% of Ki67+ cells. Finally, the group that was treated with 10 Gy and another dosage of 10 Gy five days later, expressed only 11% of Ki67+ cells (Figure 12A). With increase in ionizing radiation dosage, we see decreasing numbers of proliferating cells. Using this experimental strategy, a group of cells that are mostly proliferating, half proliferating, and mostly not proliferating were generated.

Abl localization in Ki67+ and Ki67- WT-Abl 3T3 Fibroblasts

From the 82% of Ki67+ cells (group no IR/ 0 Gy), 50% of cells expressed mostly cytoplasmic Abl (C>N) and 50% of cells expressed nuclear Abl (C=N + N>C). From the 46% of Ki67+ cells in the 2.5 Gy group, 59% of cells expressed even cytoplasmic and nuclear Abl localization. From the 11% of Ki67+ cells in the 10Gy group, all cells expressed nuclear Abl (C=N + N>C) indicating that with increasing radiation dosage, in Ki67+ cells, we see a shift towards an increased number of cells expressing nuclear Abl (Figure 12B).

The control group of 3T3 WT cells that were not irradiated (0 Gy) expressed 18% of Ki67- cells. From those Ki67- cells, we see that 67% of cells have mostly cytoplasmic localization of Abl (C>N), whereas 33% of cells express

an even distribution of Abl in both cytoplasm and nucleus (C=N). In the group irradiated with 2.5 Gy we not only have an increased percentage of Ki67- cells (54%) relative to non-irradiated (18%), but also 94% of the cells are in the cytoplasmic only (C) or mostly cytoplasmic Abl (C>N) categories. In the group that received the initial dose of 10 Gy, 89% of cells were Ki67 -, and from those cells, all of them are in the cytoplasmic only (C) or mostly cytoplasmic Abl (C>N) categories (Figure 12B).

III.

Figures

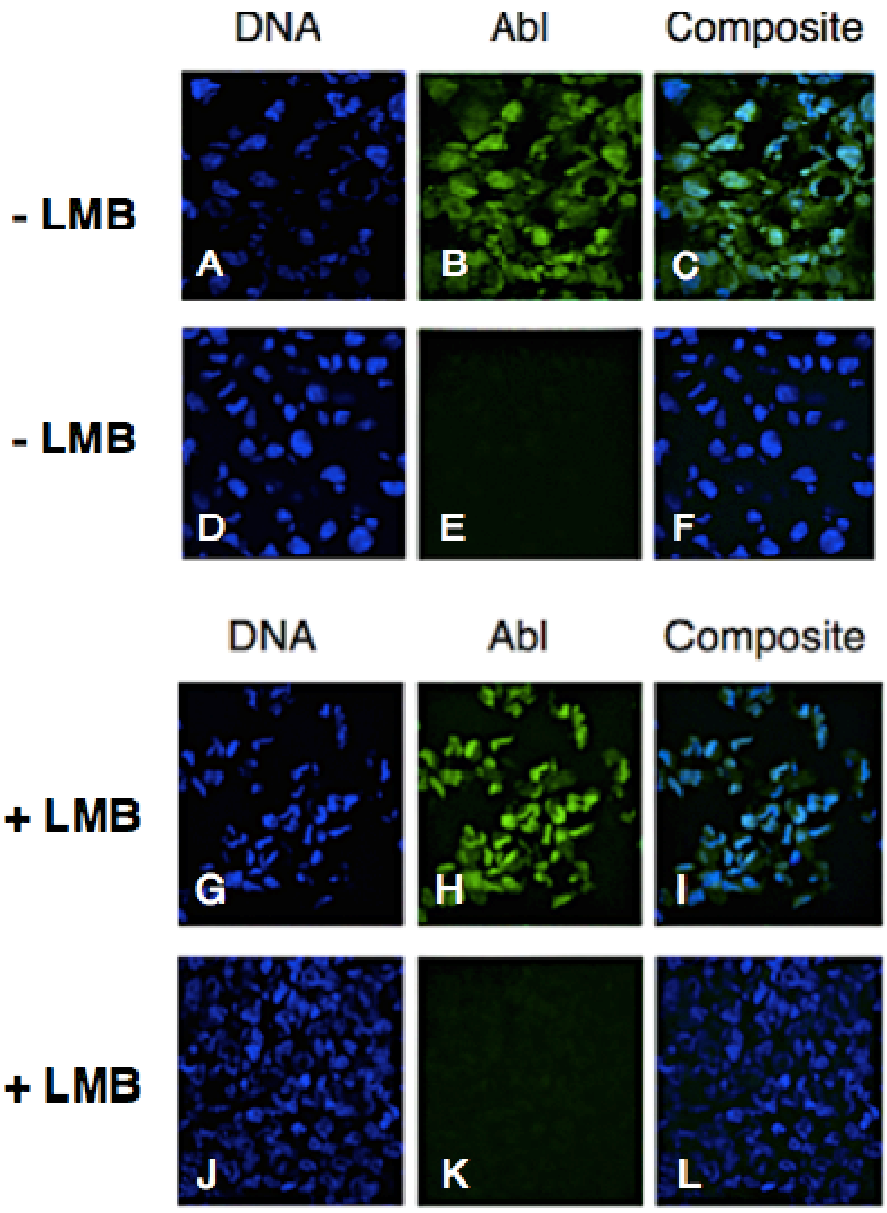

Figure 1. Fixation and Permeabilization Method for Cell Pellets of 3T3 Abl +/+ and 3T3 Abl -/- to Visualize Subcellular Abl Localization. Cell pellet sections underwent 2% PFA 10 minutes (RT), 70% EtOH 10 minutes (RT), and 0.5% Triton X-100 10 minutes (RT). Abl was stained with monoclonal anti-Abl 8E9 antibody, and cells were counterstained with Hoechst DNA dye.

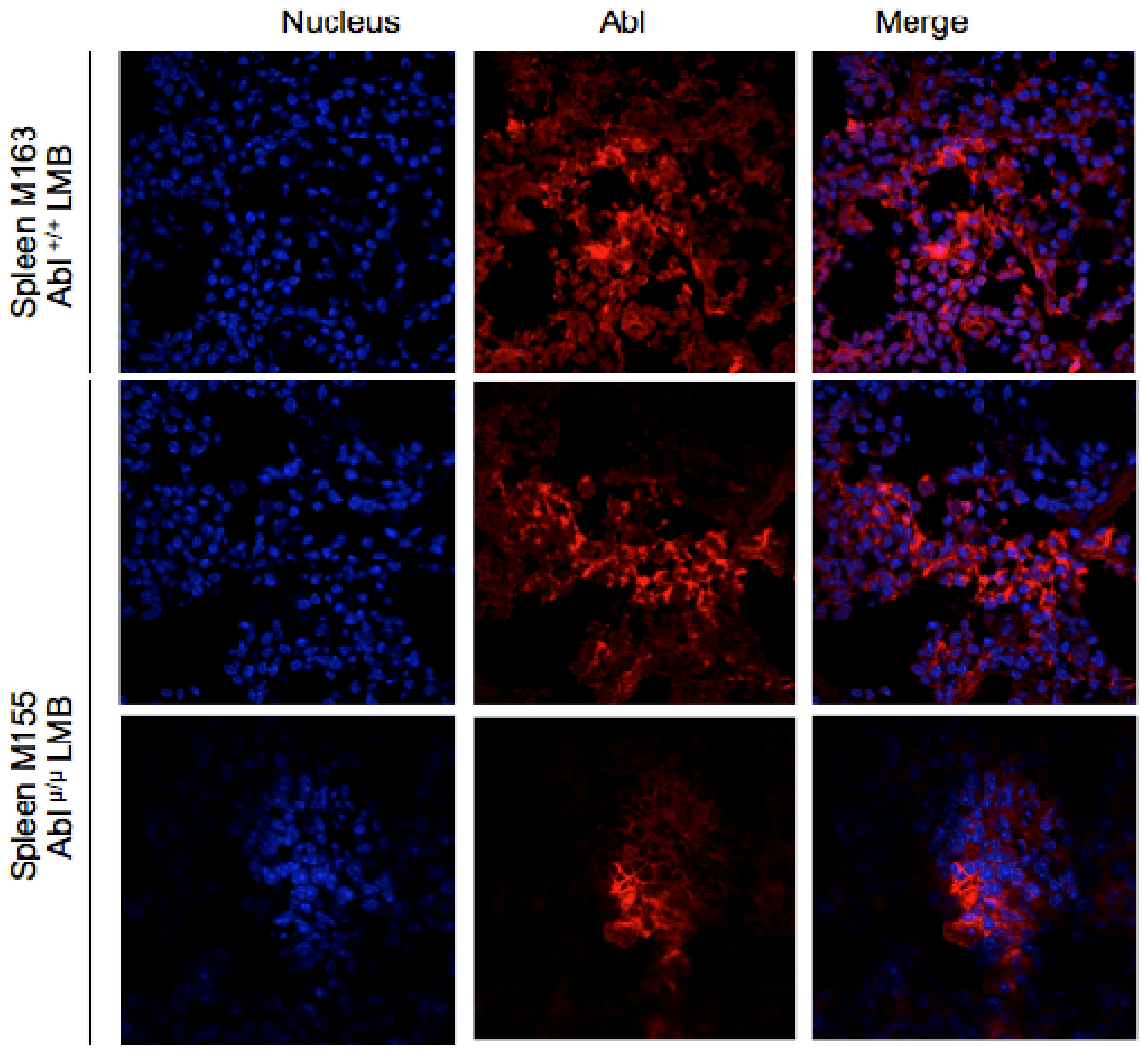

Figure 2A. Fixation and Permeabilization Method for Cell Pellets Applied on WT and μNLS Mouse Spleen Tissues. Tissue sections underwent 2% PFA 10 minutes (RT), 70% EtOH 10 minutes (RT), and 0.5% Triton X-100 10 minutes (RT). Abl was stained with monoclonal anti-Abl 8E9 antibody, and counterstained with Hoechst DNA dye.

Method #: Date	#1: 4/09/14	#2: 4/16/14	#2: 4/22/14	#3: 4/22/14	#4: 5/09/14	#5: H&E staining EDTA 5/13/14	#6: 5/24/14	#7: 5/26/14	#8: H&E staining high pH 5/29/14	#9: 6/10/14	#10: 6/23/14
Fixation	2% PFA 70% EtOH	4% PFA for 30 minutes	4% PFA fixation for 30 minutes	4% PFA fixation for 30 minutes	Drying >2 hours 4% PFA fix 30 minutes with glycine quenching step (glycine for 5 min, 10 min, 15 min)	SEE PROTOCOL &RESULTS ON PAGE:	Drying >2 hours 4% PFA 30 minutes	Drying >2 hours -20 deg methanol for 2 minutes and 30 seconds	SEE PROTOCOL &RESULTS ON PAGE:	Drying overnight. -20 degrees methanol	Drying overnight. 4% PFA for 30 minutes
Permeabilization	0.3% Triton X-100 for 15 minutes RT	0.1% Triton X-100 for 15 minutes RT	0.1% Tween 20 washes suggested by Dr. Varki	0.1% Tween 20 washes	0.1% Tween 20 washes		0.1% Tween 20 washes	0.1% Tween 20 washes		0.1% Tween 20 washes	0.1% Tween 20 washes

Figure 2B. Different Antigen Retrieval Methods. The type of fixation and permeabilization reagents and methods are listed under trial number and date.

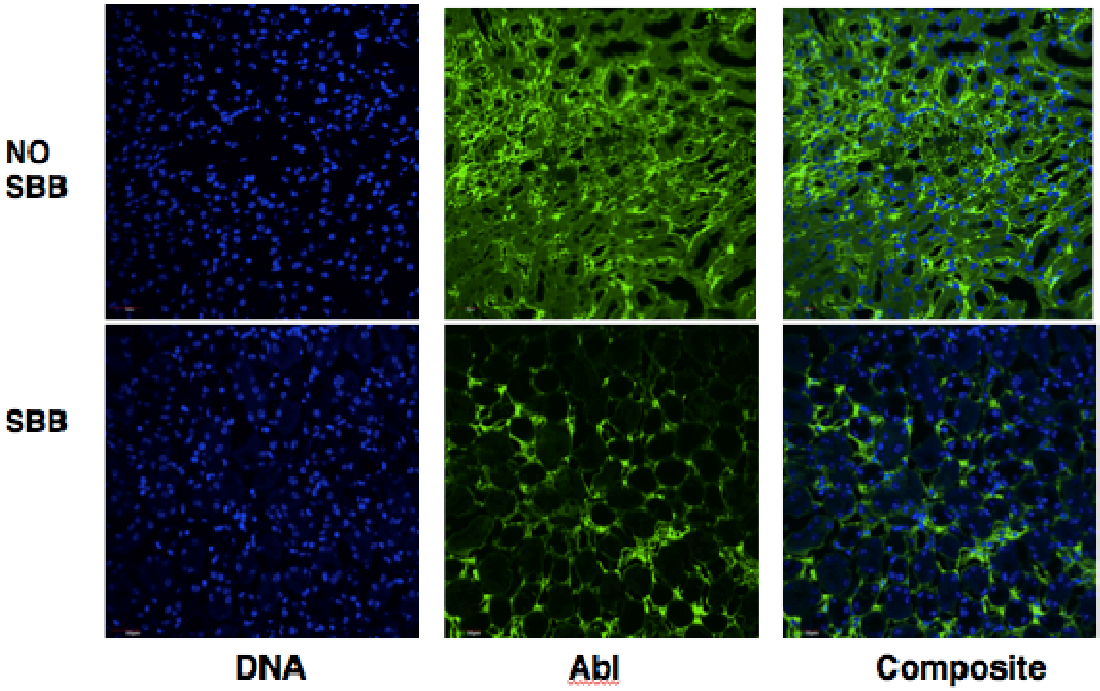

Figure 3. Application of Sudan Black B on WT Mouse Kidney Tissue. Tissue sections were permeabilized with 0.5% Triton X-100 for 15 minutes, followed by blocking with 5% BSA for 30 minutes. Abl was stained with monoclonal anti-Abl 8E9 antibody, and counterstained with Hoechst DNA dye. After Hoechst staining, 0.1%Sudan Black B was applied for 2 minutes at RT.

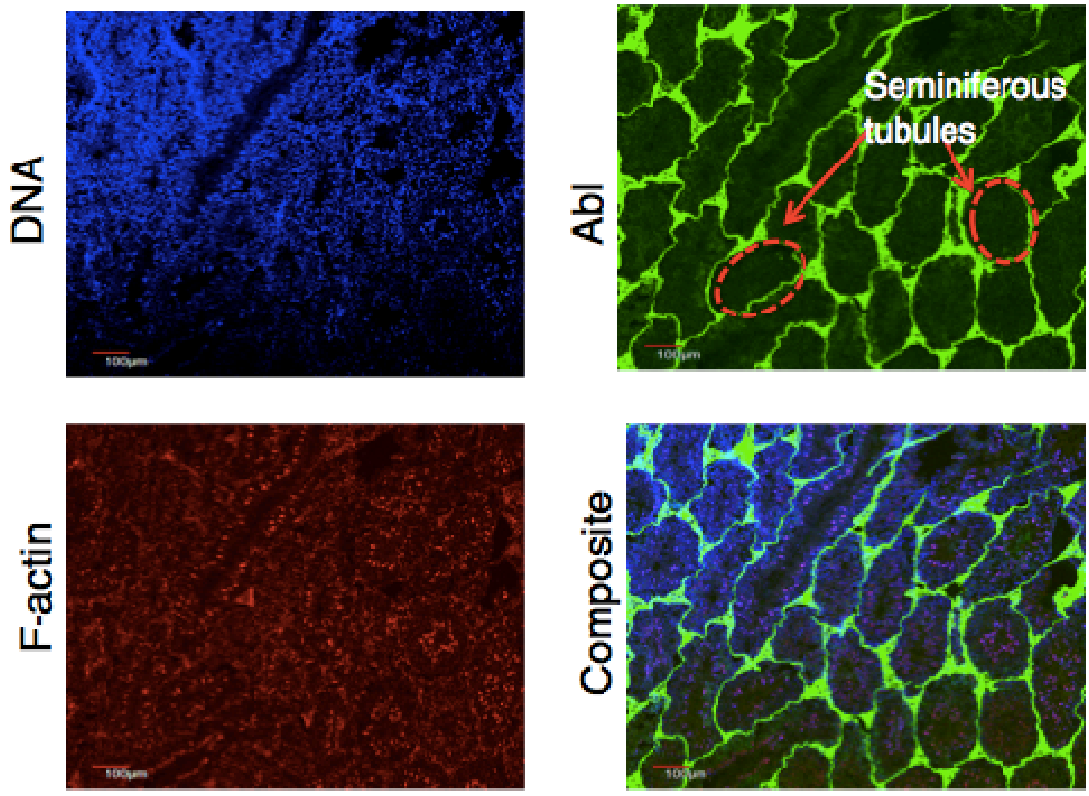

Figure 4A. WT Mouse Testis Tissue. Tissue sections were permeabilized with 0.5% Triton X-100 for 15 minutes, followed by blocking with 5% BSA for 30 minutes. Abl was stained with monoclonal anti-Abl 8E9 antibody, and counterstained with Hoechst DNA dye. F-actin was stained with Phalloidin Alexa Fluor 594 dye. Individual seminiferous tubules are visible (indicated by dotted lines).

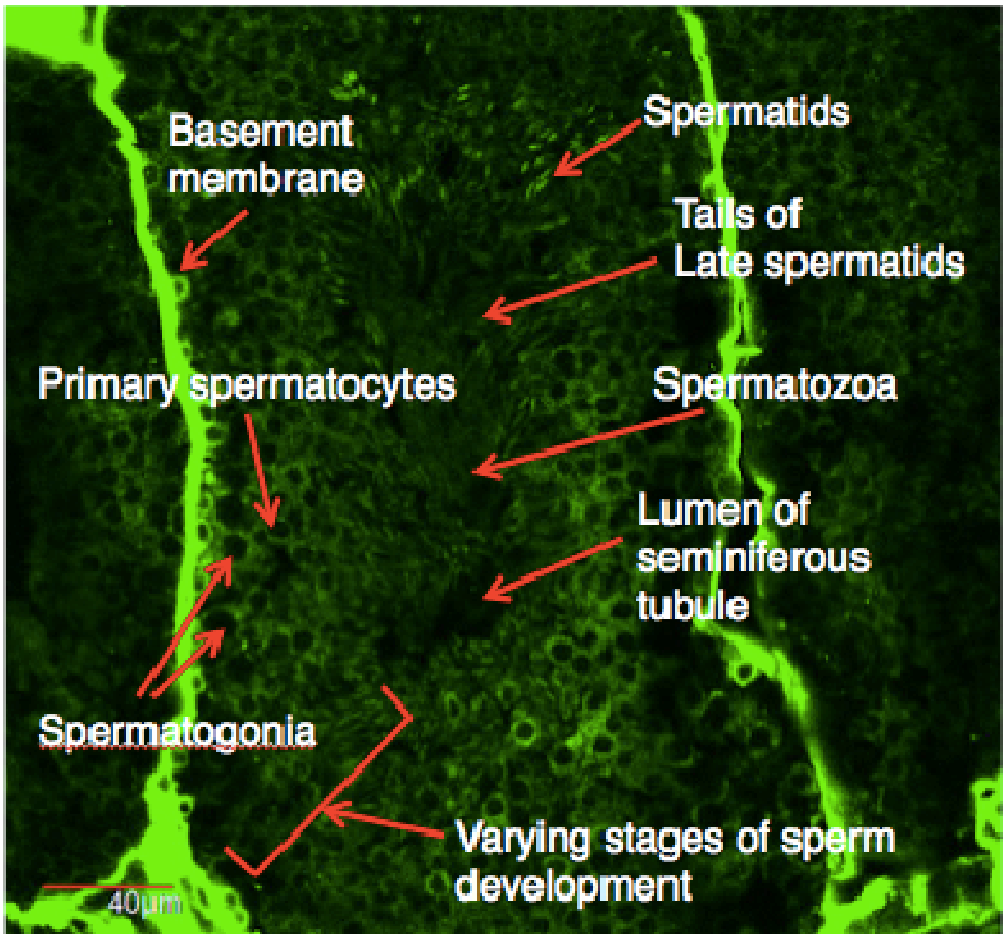

Figure 4B. Labeled Histology of Mouse Seminiferous Tubule. Tissue sections were permeabilized with 0.5% Triton X-100 for 15 minutes, followed by blocking with 5% BSA for 30 minutes. Abl was stained with monoclonal anti-Abl 8E9 antibody. This image is of Abl expression alone. Seminiferous tubule histology parts are labeled.

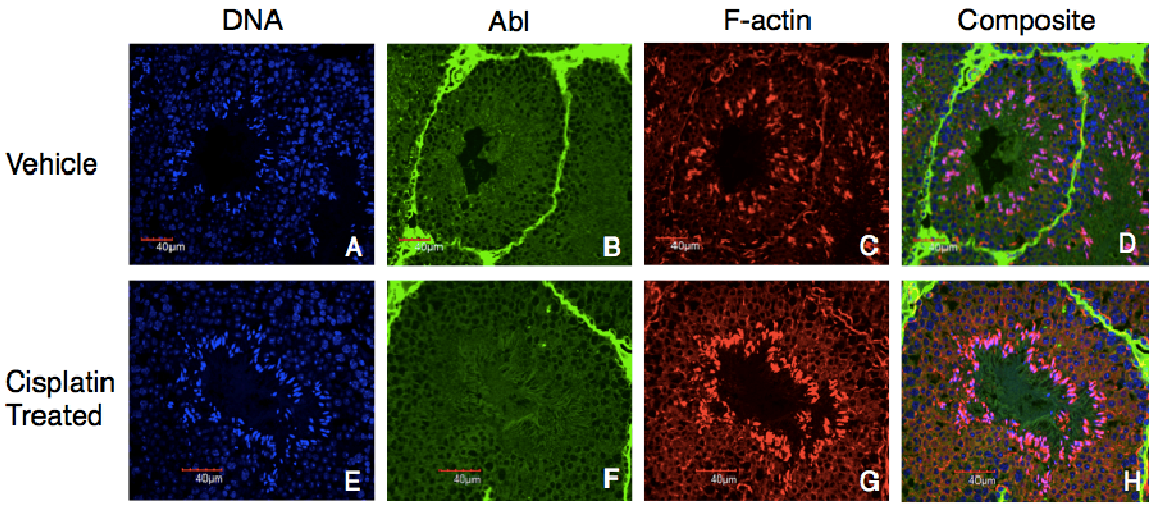

Figure 5. Abl Expression in Abl μNLS Mouse Testis Tissue. Tissue sections were permeabilized with 0.5% Triton X-100 for 15 minutes, followed by blocking with 5% BSA for 30 minutes. Abl was stained with monoclonal anti-Abl 8E9 antibody. Sections were counterstained with Hoechst DNA dye. F-actin was stained with Phalloidin Alexa Fluor 594.

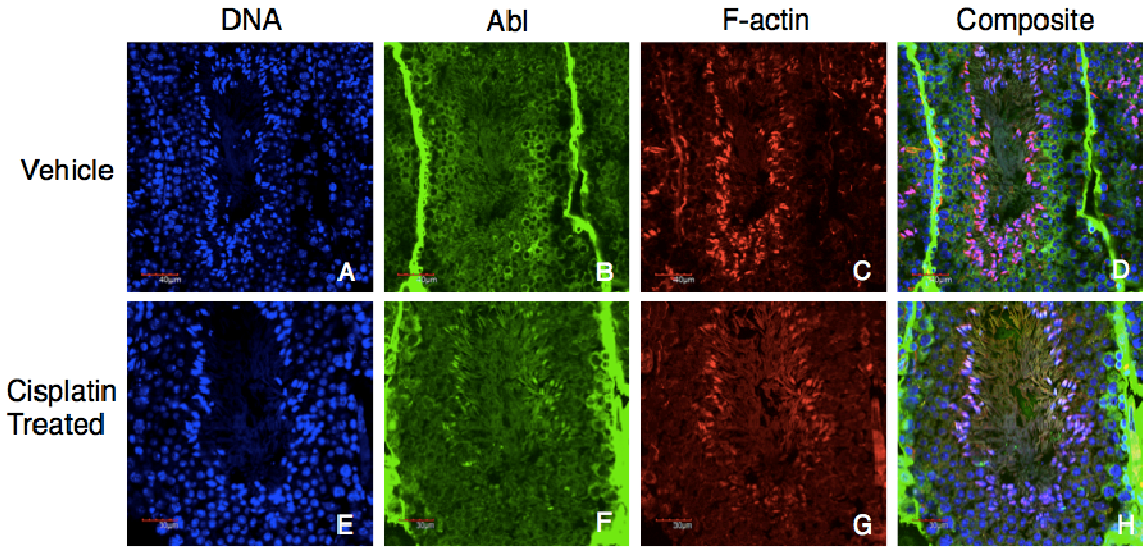

Figure 6. Abl Expression in Abl WT Mouse Testis Tissue. Tissue sections were permeabilized with 0.5% Triton X-100 for 15 minutes, followed by blocking with 5% BSA for 30 minutes. Abl was stained with monoclonal anti-Abl 8E9

antibody. Sections were counterstained with Hoechst DNA dye. F-actin was stained with Phalloidin Alexa Fluor 594.

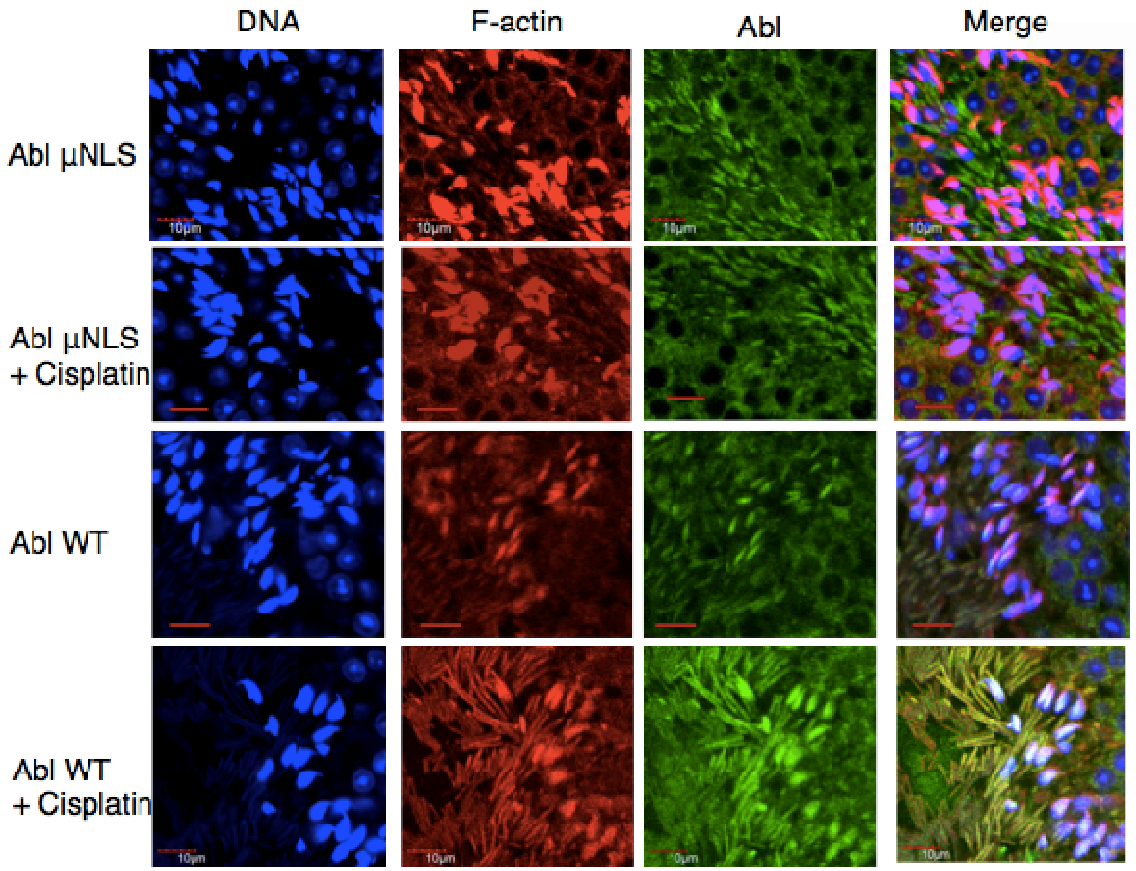

Figure 7. Magnification of Abl expression in Abl WT and Abl μNLS Mouse Spermatids. Tissue sections were permeabilized with 0.5% Triton X-100 for 15 minutes, followed by blocking with 5% BSA for 30 minutes. Abl was stained with monoclonal anti-Abl 8E9 antibody. Sections were counterstained with Hoechst DNA dye. F-actin was stained with Phalloidin Alexa Fluor 594. Co-localization of DNA (450 nm), F-actin (594 nm), and Abl (488 nm) is indicated by the white-pink color in Merge panels.

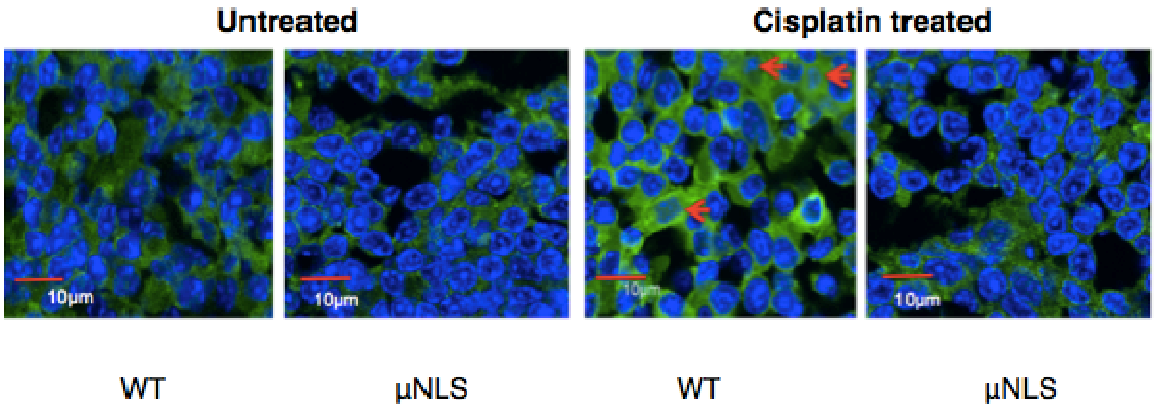

Figure 8. Magnification of Co-localization of DNA and Abl in Abl WT and Abl µNLS Mouse Spleen Tissue in Red Pulp. Tissue sections were permeabilized with 0.5% Triton X-100 for 15 minutes, followed by blocking with 5% BSA for 30 minutes. Abl was stained with monoclonal anti-Abl 8E9 antibody. Sections were counterstained with Hoechst DNA dye. Nuclear Abl expression in cisplatin treated WT-Abl mouse spleen tissue cells are indicated by red arrows.

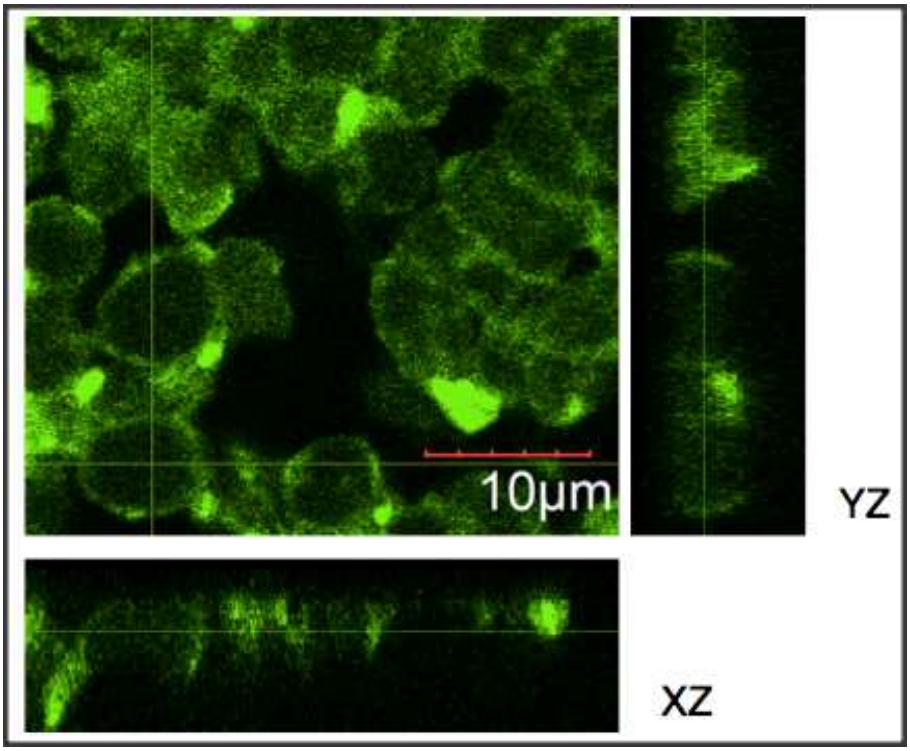

Figure 9A. Z-stack of Abl Expression in Abl- μNLS Mouse Spleen Tissue Red Pulp. Tissue sections were permeabilized with 0.5% Triton X-100 for 15 minutes, followed by blocking with 5% BSA for 30 minutes. Abl was stained with monoclonal anti-Abl 8E9 antibody. Z-stack is comprised of 41 slices; each slice is 0.30 μm in depth.

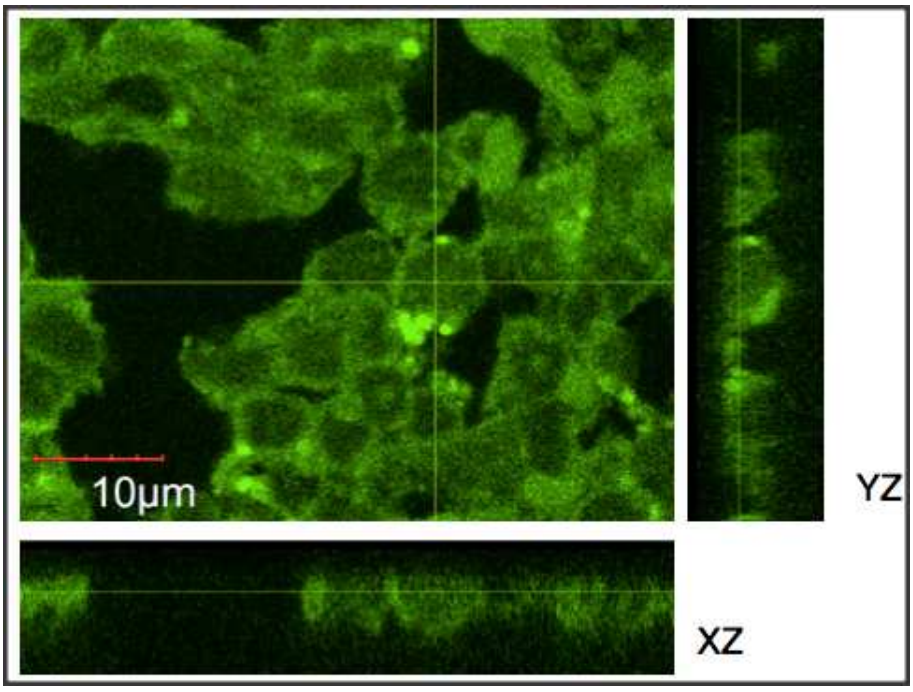

Figure 9B. Z-stack of Abl Expression in Abl- WT Mouse Spleen Tissue Red Pulp. Tissue sections were permeabilized with 0.5% Triton X-100 for 15 minutes, followed by blocking with 5% BSA for 30 minutes. Abl was stained with monoclonal anti-Abl 8E9 antibody. Z-stack is comprised of 45 slices; each slice is 0.30 µm in depth.

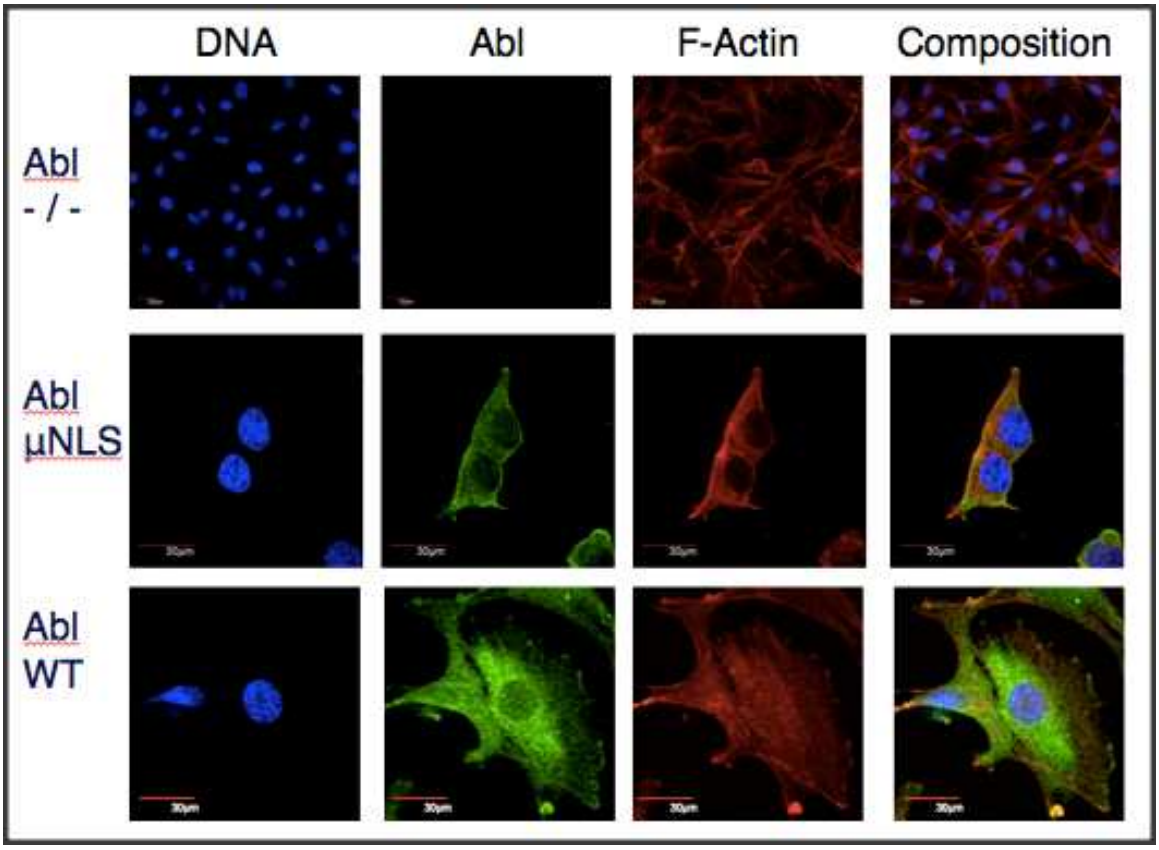

Figure 10. Abl staining in Abl null, Abl- µNLS, and Abl-WT 3T3 Fibroblasts. Representative images of Abl null, Abl- µNLS, and Abl-WT 3T3 fibroblasts in their steady state. Abl-µNLS cells express exclusive cytoplasmic Abl localization. Abl-WT cells express both nuclear and cytoplasmic Abl localization.

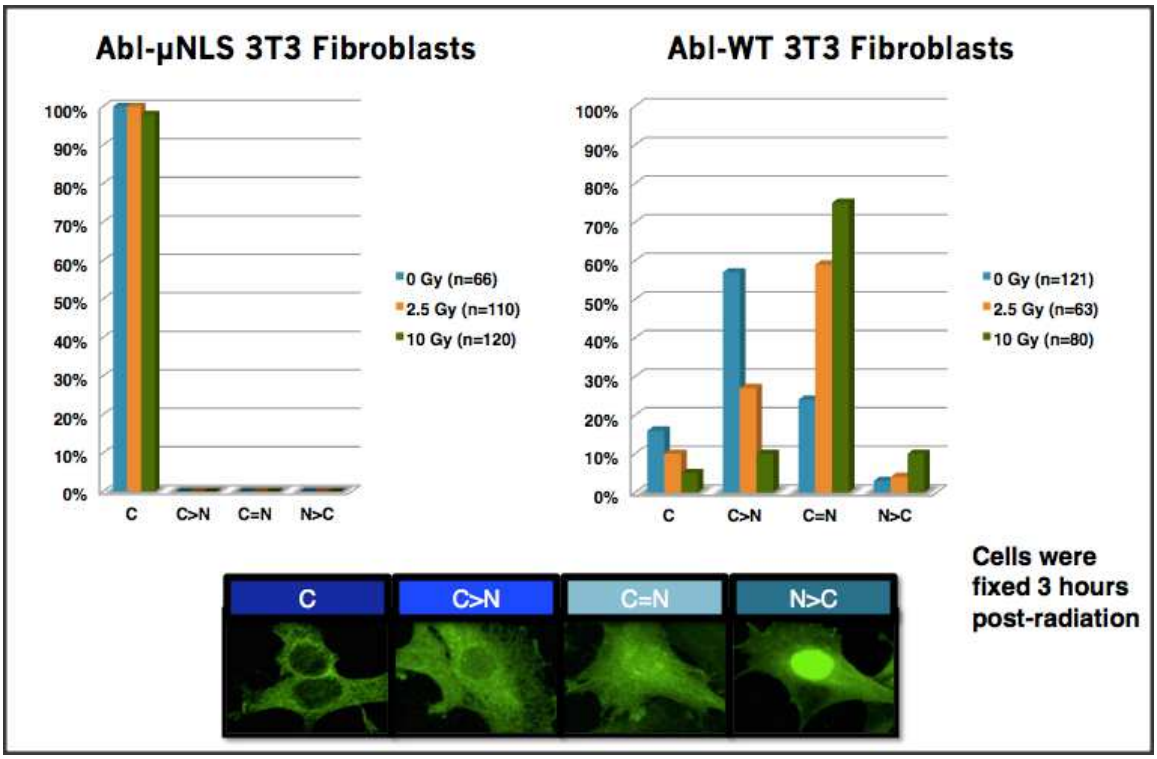

Figure 11. Effect of Ionizing Radiation on Abl-WT and Abl- μNLS 3T3 fibroblasts. Cells were exposed to no radiation (0 Gy), 2.5 Gy, or 10 Gy. Cells were fixed 3 hours post-radiation for immunofluorescence.

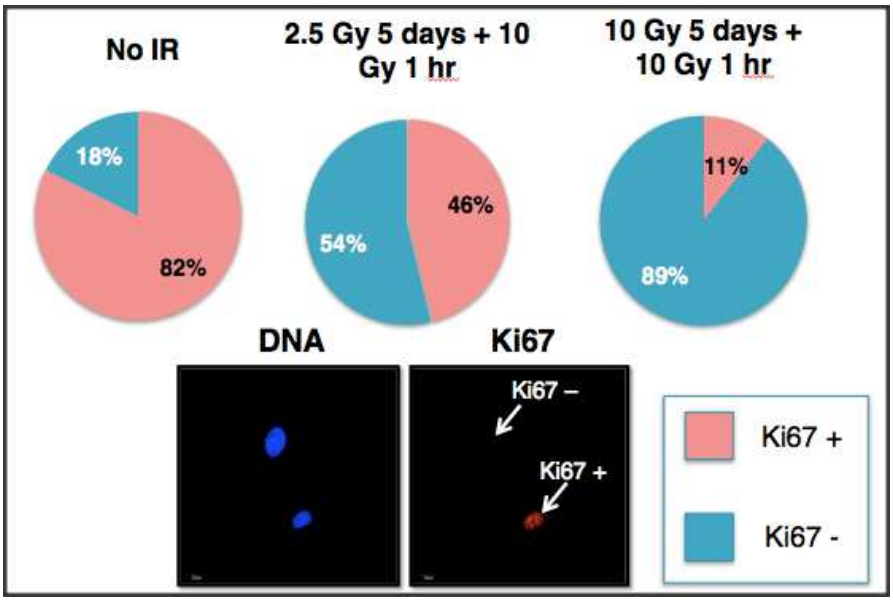

Figure 12A. Effect of Ionizing Radiation on Ki67 Expression in Abl-WT 3T3 Fibroblasts. Abl-WT 3T3 fibroblasts received an initial dosage of 2.5 Gy or 10 Gy IR, and after five days of culture they received a final dosage of 10 Gy. Cells were stained with Ki67, a proliferation marker, and counterstained with Hoechst DNA dye.

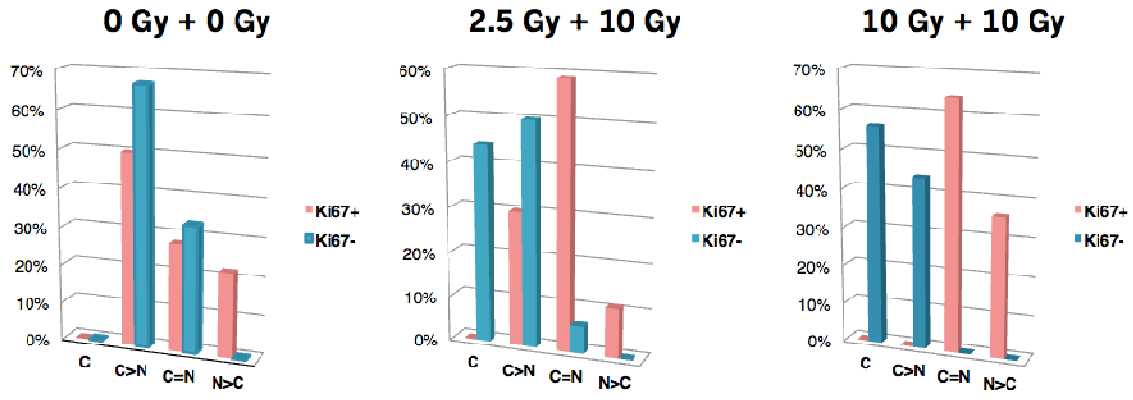

Figure 12B. Abl localization in Ki67+ and Ki67 - WT-Abl 3T3 Fibroblasts. The table from Figure 13A has been made into bar graphs. Abl-WT 3T3 fibroblasts received an initial dosage of 2.5 Gy or 10 Gy ionizing radiation, and after five days of culture they received a final dosage of 10 Gy. Cells were stained with Ki67, a proliferation marker, and counterstained with Hoechst DNA dye.

IV.
Discussion

Abl tyrosine kinase, unlike other tyrosine kinases, is found both in the cytoplasm and nucleus. It has three nuclear localization signals (NLS) and one nuclear export signal (NES) that allows it to shuttle between the nucleus and cytoplasm (9). In response to extracellular signals such as cytokines or microbial infections, Abl tyrosine kinase is activated in the cytoplasm and regulates actin dynamics. In response to DNA-damaging agents such as cisplatin, doxorubicin, and ionizing radiation (IR), there is an accumulation and activation of nuclear Abl through ATM and DNA-PK mechanisms which then induces intrinsic apoptosis by triggering the p53 and p73 family of transcription factors (8, 1). By inducing DNA damage in both Abl WT and Abl- μNLS mice using cisplatin injections (a platinum based chemotherapy drug), our lab has not only confirmed that DNA damage induces nuclear accumulation and activation of Abl tyrosine kinase leading to intrinsic apoptosis, but also that cisplatin-induced apoptosis is defective in Abl- μNLS mice (8). This demonstrates that nuclear localization and activation of Abl tyrosine kinase is necessary for DNA-damage induced intrinsic apoptosis. Thus, depending on the subcellular localization of where Abl is activated, this kinase has the potential to stimulate cell death or cell survival.

Because Abl's biological effect in the cell is determined by its subcellular localization, visualization of Abl is both vital and useful. There are currently, however, no publications that can visualize Abl in tissues through either branch of immunohistochemistry: immunofluorescence and hematoxylin and eosin (H&E) staining. In our lab many attempts were made at visualizing Abl through H&E staining methods, and have found the results unsuccessful. This may be

due to the harsh nature of H&E antigen retrieval methods (high or low pH solutions and/or heating), which may denature the SH2 domain – the epitope our monoclonal anti-Abl 8E9 antibody binds to. Thus the objective was to create an optimal immunofluorescence protocol that yields high preservation of cellular structures, antigen accessibility, and an accurate expression and distribution of Abl tyrosine kinase as close as possible to its *in vivo* state.

Before using tissue sections, cell pellet sections were made from 3T3 Abl-WT and 3T3 Abl null fibroblasts to use as controls to test different antibody dilutions and antigen retrieval methods. Generating cell pellet sections provided thicker samples to work with relative to monolayer cells, mimicking tissue sections. The fixation and permeabilization method that works for monolayer cells did not work for cell pellet sections, confirming that thicker sample size requires a different fixation and permeabilization method. We found that cell pellets require fixation with 2% PFA (10 minutes RT) and post-fixation with 70% ethanol (10 minutes RT). The 3T3 Abl-WT cell pellet sections expressed both cytoplasmic and nuclear Abl, but with the application of Leptomycin B (LMB), the cells exhibited nuclear accumulation of Abl. These results parallel to Abl expression in monolayer Abl-WT cells. The 3T3 Abl-null cell pellet sections expressed no Abl, affirming that the Abl expression we see in 3T3 Abl-WT cells is accurate. With this fixation method we can utilize immunofluorescence to visualize Abl in cell pellet sections.

In order to attain mouse tissue sections, we first harvested the organs, embedded them in 100% optimal cutting temperature compound (OCT), snap-

froze them in a dry ice-over-isopentane bath, and had the frozen tissues sectioned into ~20 μm slices. Using these mouse tissue sections, we first tried the fixation and permeabilization method used on cell pellet sections. The stained tissue revealed poor morphology with high background fluorescence. Assuming the problems are due to fixation and permeabilization problems, several different fixation and permeabilization methods were endeavored and yielded similar results: poor tissue integrity and high background “noise” (Figure 2B). Some of the fixation methods that were endeavored include: 4% PFA for 30 minutes, overnight dehydration with 4% PFA and glycine quenching, overnight dehydration with precooled -20 °C methanol, and combination of methanol and acetone for 2 minutes each. All of the antigen retrieval methods, however, were unsuccessful. I then hypothesized that this was due to the poor preservation of tissue and not due to the antigen retrieval method. For example, the poor tissue morphology may be due to inadequate fixation (under-fixation or over-fixation). It may also be due to the formation of ice crystals within the OCT-embedded tissue, which would result in splitting of tissue (seen in Figure 2A). To resolve these issues, a new protocol was created that incorporates the fixation step immediately after harvesting the mice organs, and also includes a cryoprotection step, which utilizes sucrose to prevent the formation of ice crystals within the tissue.

To resolve the issue of high background fluorescence, we executed the following controls: 8E9 antibody only, secondary Alexa Fluor 488 antibody only, and lastly 5% BSA only. This was to ensure that the high background

fluorescence was not due to missteps such as insufficient washing, too high of an antibody dilution, etc. Upon confirmation that the controls expressed minimum to no fluorescence, we then hypothesized that the high background may be due to autofluorescence from naturally fluorescing structures. We came upon this hypothesis because the minimum fluorescence expressed in controls arose from basement membranes, connective tissue (collagen, elastin), and blood vessels (elastin): all three which emit natural fluorescence.

Sudan Black B, a lysochrome or fat soluble dye, was used to diminish natural fluorescence. There was still high expression of Abl in basement membranes and capsule tissues, but Sudan Black B significantly diminished the high background allowing identification of individual cells and structures. In the future, a confocal that can read emission waves and thus distinguish natural fluorescence from antibody signals will be used to image Abl expression in mouse tissues.

The tissue sections generated with the new protocol were whole and structural components were identifiable with Abl staining alone (Figure 4B). This indicates that Abl tyrosine kinase is truly a ubiquitously expressed protein, and a pool of a cytoplasmic Abl is found in all cells.

From staining Abl-WT and Abl- μNLS mouse testis tissues, we found that Abl- WT mice spermatids expressed nuclear Abl expression and also Abl expression in their tails. Unlike monolayer cells, this is the first time we have seen high expression of nuclear Abl without a DNA-damaging agent. Abl- μNLS mouse spermatids, however, did not express nuclear Abl expression and only

expressed Abl in their tails. Furthermore, in Abl- μNLS mouse testis tissues, the spermatogonia, primary spermatocytes, and all other cells of spermatogenesis expressed only cytoplasmic Abl. Cisplatin treated Abl- μNLS mouse testis tissues exhibited similar characteristics, and only Abl localized only in the cytoplasm (Figure 5 Panel F). The lack of nuclear Abl in Abl-μNLS spermatids and all other cells in stages of spermatogenesis parallels to the exclusive cytoplasmic Abl expression in Abl-μNLS monolayer cells. In Abl- WT mouse testis tissues, untreated, the spermatogonia and primary spermatocytes expressed only cytoplasmic Abl (Figure 6 Panel B). With cisplatin treatment, however, there is an increase in number of spermatids with high expression of nuclear Abl (Figure 7), and there is also expression of nuclear Abl in spermatogonia and primary spermatocytes (Figure 6 Panel F). The increase in the number of cells with nuclear expression of Abl in response to DNA damage corresponds to what occurs in monolayer cells. This indicates that what DNA damage results in the accumulation and activation of Abl *in vivo*. The difference between the Abl-μNLS mouse tissue cells and Abl-WT mouse tissue cells confirm that the fluorescence observed is Abl. Furthermore, because spermatogonia and spermatocytes are cells in the proliferation phase of spermatogenesis, we hypothesized that upon DNA damage, Abl accumulates in the nucleus only in proliferating cells.

Abl-WT and Abl- μNLS mouse spleen tissues were also stained for Abl and DNA. All cells in Abl-WT mouse spleen tissues, untreated, expressed exclusively cytoplasmic Abl with a few cells that seem to show some expression of nuclear Abl. Abl-WT spleen tissues treated with cisplatin, however, expressed

cells with accumulation of nuclear Abl. In cisplatin treated Abl-WT mouse spleen tissues, there were a higher number of cells with nuclear Abl expression in red pulp in comparison to white pulp. In Abl- μNLS untreated spleen tissues there was expression of only cytoplasmic Abl. Abl- μNLS spleen tissues treated with cisplatin exhibited no expression of nuclear Abl. To confirm that the Abl nuclear fluorescence is in the nucleus, z-stacks were taken of both cisplatin treated Abl-μNLS spleen tissue red pulp cells and cisplatin treated Abl-WT spleen tissue red pulp cells. The compilation of 0.30 μm slices show the cells from the sides (yz or xz) .The z-stack of Abl- μNLS spleen cells display no nuclear Abl expression in both yz and xz panels. In the cisplatin treated Abl-WT spleen cells, the yz panel displays 2/3 cells with nuclear Abl and the xz panel displays 1/3 cells (the cell selected by both x and y axis) with nuclear Abl. This indicates that cisplatin does have a DNA damaging effect in mouse spleen tissues, and induces nuclear Abl accumulation in Abl-WT spleen cells. The accumulation of nuclear Abl only in Abl-WT spleen cells parallels to what is described in literature for monolayer cells (8). Most cells in cisplatin treated Abl-WT spleen tissue and testis tissue expressed only cytoplasmic Abl. Because of this heterogeneity and from what we observed in mouse testis tissue, we hypothesized that upon DNA damage, Abl accumulates in the nucleus only in proliferating cells.

To investigate if Abl accumulates in the nucleus of only proliferating cells in response to DNA damage, we chose 3T3 fibroblast monolayer cells as the experimental system. In steady state Abl-WT 3T3 fibroblasts, Abl is expressed in both cytoplasm and nucleus. In steady state Abl- μNLS 3T3 fibroblasts there is

only expression of cytoplasmic Abl. Before observing ionizing radiation as a DNA-damaging agent in cells with a double dose of radiation, we first observed the effects of ionizing radiation on Abl localization in Abl- WT and Abl-μNLS 3T3 cells from a single dose of radiation (2.5 Gy and 10 Gy). Abl- μNLS cells irradiated with 2.5 Gy or 10 Gy did not differ from their steady state, and expressed only cytoplasmic Abl (Figure 11). Upon DNA damage, Abl in Abl-μNLS cells cannot import into the nucleus due to the inactivation of the three nuclear localization signals, thus we see only cytoplasmic expression of Abl. When Abl-WT 3T3 cells were not radiated, 16% of cells were cytoplasmic (C), but most cells had both cytoplasmic and nuclear Abl (C>N [57%] and C=N [24%]) (n=121) (Figure 11). Thus without radiation, we see that Abl tyrosine kinase is localized both in the cytoplasm and nucleus. When the Abl-WT 3T3 cells were radiated with 2.5 Gy, there is an increase in the number of cells with even distribution of Abl expression in both cytoplasm and nucleus (C=N [59%]). This confirms that in response to DNA damage, there is localization and activation of Abl in the nucleus. With a 10 Gy dose, the number of cells with nuclear Abl expression increases, we see that the cells under the categories C only and C>N have decreased whereas the cells under the categories C=N and N>C have increased in percentage. This trend of increasing dosage of ionizing radiation and thus increasing DNA damage resulting in increasing number of cells with nuclear Abl expression confirms that Abl is localized and activated in the nucleus in response to DNA damage. This also confirms that nuclear localization of Abl is not required

for cells to proliferate, because Abl- μNLS 3T3 cells are able to proliferate without the nuclear accumulation of Abl.

It has been observed in this lab and described in literature, that cells irradiated with a 10 Gy dosage are no longer able to proliferate. Thus for this experiment, the strategy was to create a group of cells that no longer proliferate by radiating them with a primary dose of 10 Gy, then after 5 days of culture, the cells were radiated with a secondary dose of 10 Gy. The primary dose will result in many dead and no-longer proliferating cells. Because so many cells result in apoptosis after being irradiated with 10Gy, a group of cells that are radiated with a primary dose of 2.5 Gy was added to the experiment. After 5 days of culture, we radiated the cells with a secondary dose of 10 Gy, which was executed in order to induce DNA damage and thus the accumulation of nuclear Abl (as we saw in 3T3 Abl-WT cells radiated with a single dose of 10 Gy Figure 11). Figure 12A shows that with increasing ionizing radiation strength, we have a decrease in the number of proliferating cells. With no radiation, 82% of the Abl-WT cells still proliferated, whereas a 2.5 Gy + 10 Gy combination resulted in 46% of proliferative cells, and lastly a combination of 10 Gy + 10 Gy resulted in only 11% of proliferative cells. In the Ki67+ cells, we see that with an increase in ionizing radiation dosage there is a shift towards an increase in the number of cells expressing nuclear Abl (Figure 12B). In Ki67- cells, we observed that with increase in ionizing radiation dosage there is a shift towards an increase in the number of cells that express exclusively cytoplasmic Abl. These results confirm

that in response to DNA damage, Abl accumulates in the nucleus of proliferating 3T3 Abl-WT cells.

The next question will be to see if our *in vitro* observation is also true *in vivo*. Towards this aim, one will need to investigate the nuclear accumulation of Abl in proliferating vs. non-proliferating cells in mouse tissues. By co-staining for Ki67 and Abl in mouse tissues before and after exposure of mice to ionizing radiation, we can determine if only the Ki67-positive cells will express nuclear Abl following radiation. It is known that nuclear localization and activation of Abl tyrosine kinase stimulates DNA damage-induced apoptosis. The finding from this thesis research suggests that nuclear localization and activation of Abl by DNA damage only occur in proliferative cells. Taken together, these findings can provide an explanation for why proliferating cells such as cancer cells die in response to radiation and genotoxic drugs, whereas senescent cells such as neurons and cardiac muscle cells do not undergo this death response and therefore are not killed by radiation and genotoxic drugs in cancer patients undergoing radiation and chemotherapy.

V.

Materials and Methods

Cell culture and transfection

BOSC23 cells were maintained in Dulbecco's Modified Eagle Mediumm (DMEM) supplemented with 10% fetal bovine serum (FBS) and 1% penicillin and streptomycin. BOSC34 cells were grown to 90% confluence in 6cm plates, and liposome mediated transfection with plasmids was executed using Genetran reagent following the manufacturer's instructions and incubated for 24 hours. The supernatant was then collected and 3T3 μNLS cells were infected. Antibiotic selection was completed using hygromycin.

Induction of DNA damage in Cisplatin treated mice

For cisplatin treatments, adult Abl WT and Abl μNLS mice were given a single intraperitoneal injection of pharmacological grade cisplatin at 20mg/kg body weight. Mice were euthanized with carbon dioxide asphyxiation.

Induction of DNA damage in irradiated 3T3 cells

Approximately 150,000 3T3 cells were seeded into each well, of a 24 well plate, and irradiated at 2.5 Gy or 10 Gy.

Tissue Immunofluorescence

All organs were cut into size similar to halves of kidneys, and placed immediately into cold PBS. Each organ was then transferred into 500 microliters of freshly prepared 4% paraformaldehyde, and left for 16 hours RT. Each was

then transferred into 15% sucrose and PBS for 24 hours at 4° C. Organs were then transferred into 30% sucrose in PBS for 24 hours 4° C, replacing it with fresh 30% sucrose 3 times throughout the 24 hours. Half of the 30% sucrose was exchanged for 30% OCT in PBS, making it 1:1 30% sucrose/OCT (1-2 hours 4° C). The organs were then placed in 100% OCT in vinyl molds for 1 hour at 4° C, then snap frozen in isopentane over dry ice.

Sectioned 5 μm tissues were dehydrated overnight, and then placed in 0.5% Triton X-100 solution in PBS for 20 minutes room temperature. They were blocked with 5% BSA for 30 minutes, followed by incubation with anti-Abl (8E9) antibody (30 μg/mL) for 1 hour at 37° C, followed by ALEXA fluor-488 (Invitrogen)-chicken anti-mouse (1:500) for 30 minutes at 37° C. Nuclei were stained with Hoechst 3342. Tissues were then stained with 0.1 % Sudan Black B.

Cell pellet Immunofluorescence

Approximately 100 million cells of 3T3 Abl WT and 3T3 Abl -/- cells were grown, and spun into pellets. Each pellet was embedded in OCT and snap frozen in isopentane over dry ice. 5 μm sections were fixed in 2% paraformaldehyde for 10 minutes, followed by 70% EtOH for 10 minutes, then permeabilized with 0.5% Trtion-X-100 for 10 minutes. They were blocked with 5% BSA for 30 minutes, followed by incubation with anti-Abl (8E9) antibody (30 μg/mL) for 1 hour at 37° C, followed by ALEXA fluor-488 (Invitrogen)-chicken anti-mouse (1:500) for 30 minutes at 37° C. Nuclei were stained with Hoechst 3342.

Cells monolayer Immunofluorescence

Cells were grown on Poly-L-lysine treated cover slips. Cells were fixed with freshly prepared 4% paraformaldehyde for 15 minutes, permeabliized with 0.5% Trtion X-100 for 15 minutes, and blocked with 5% BSA for 30 minutes. The cells were then incubated with anti-Abl (8E9) antibody (30 µg/mL) for 1 hour at 37° C, followed by ALEXA fluor-488 (Invitrogen)-chicken anti-mouse (1:500) for 30 minutes at 37° C. Nuclei were stained with Hoechst 3342.

VI.

References

1. Gong, J. G., Costanzo, A., Yang, H.-Q., Melinos, G., Kaelin Jr., W. G., Levrero, M., and Wang, J. Y. J. “The tyrosine kinase c-Abl regulates p73 in apoptotic response to cisplatin-induced DNA damage.” *Nature* 399 (1999): 806-809.

2. Hayat, M.A. “Methods of Cancer Diagnosis, Therapy and Prognosis Breast Carcinoma.” (Springer, 2008).

3. Kharbanda, S., Pandey, P., Jin, S., Inoue, S., Bharti, A., Yuan, Z.-M., Weichselbaum, R., Weaver, D., and Kufe, D. “Functional interaction between DNA-PK and c-Abl in response to DNA damage.” *Nature* 386, (1997): 732–735.

4. Odell, I. D., and Cook, D. (2013). “Immunofluorescence Techniques.” Journal of Investigative Dermatology 133, e4.

5. Preyer, M., Shu, C.-W., and Wang, J. Y. J. “Delayed activation of Bax by DNA damage in embryonic stem cells with knock-in mutations of the Abl nuclear localization signals.” *Cell Death and Differentiation* 14, no.6 (2007): 1139–1148.

6. Schnell, S. A., Staines, W. A. & Wessendorf, M. W. “Reduction of Lipofuscin-like Autofluorescence in Fluorescently Labeled Tissue.” *Journal of Histochemistry & Cytochemistry* 47**,** (1999): 719–730.

7. Shafman, T., Khanna, K. K., Kedar, P., Spring, K., Kozlov, S., Yen, T., Hobson, K., Gatei, M., Zhang, N., Watters, D., et al. “Interaction between ATM protein and c-Abl in response to DNA damage.” *Nature* 387, (1999): 520–523.

8. Sridevi, P., Nhiayi, M. K., and Wang, J. Y. J. “Genetic disruption of Abl nuclear import reduces renal apoptosis in a mouse model of cisplatin-induced nephrotoxicity.” *Cell Death and Differentiation* 20, no.7 (2013): 953–962.

9. Taagepera, S. *et al.* “Nuclear-cytoplasmic shuttling of C-ABL tyrosine kinase.” *Proceedings of the National Academy of Sciences* 95, no.13 (1998): 7457–7462.

10. Tybulewicz, V. L., Crawford, C. E., Jackson, P. K., Bronson, R. T., and Mulligan, R. C. “Neonatal lethality and lymphopenia in mice with a homozygous disruption of the c-abl proto-oncogene.” *Cell*, 65, no.7 (1991): 1153–1163.

11. Wang, J.Y. “Regulation of cell death by the Abl tyrosine kinase.” *Oncogene* 19, no.49 (2000): 5643 – 5650.

12. Woodring, P. J., Hunter, T., and Wang, J.Y. “Regulation of F-actin-dependent processes by the Abl family of tyrosine kinases.” *Journal of Cell Science*, (2003): 2613–2626.

13. Vigneri, P. & Wang, J. Y. J. “Induction of apoptosis in chronic myelogenous leukemia cells through nuclear entrapment of BCR-ABL tyrosine kinase.” *Nature Medicine* 7, no. 2 (2001): 228–234.

14. Zhu, J., and Wang, J. Y. “Death by Abl: A Matter of Location.” *Current Topics in Developmental Biology* 59, (2004): 165–19